Mechanism for photon emission from Au nano-hemispheres induced by scanning tunneling microscopy

Yish-Hann Liau and Norbert F. Scherer[a)]
Department of Chemistry, the James Franck Institute and Materials Research Science and Engineering Center, University of Chicago, Chicago, Illinois 60637

(Received 23 December 1998; accepted for publication 27 April 1999)

The photon emission yield observed in scanning tunneling microscopy (STM) measurements of Au hemispheroid-decorated thin films is used to elucidate the interaction of tunneling electrons with local surface plasmon modes. The photon emission probability is found to depend on the surface feature size. The agreement of a model calculation with the experimental results demonstrates that inelastic electron tunneling is the dominant mechanism of STM-induced plasmon excitation for 10–60 nm size metallic features. © *1999 American Institute of Physics.* [S0003-6951(99)00325-3]

Surface plasmons, surface electromagnetic waves that can be created by electron or photon excitation, are sensitive to local geometry of surfaces and thus are valuable tools for probing surface properties.[1,2] Surface plasmons are responsible for the enhancement of Raman scattering of molecules on surfaces,[3] photoelectron emission from rough metal surfaces,[4,5] and also photon emission from metal–insulator–metal tunneling junctions.[6] These studies, however, generally report surface averaged responses that are not directly correlated with surface microscopic structure.

Scanning tunneling microscopy (STM)[7] is widely used to measure surface topography with atomic resolution but can also serve as a microscopic electron source of constant intensity through the tip apex. By combining STM with photon detection one can study the relation between electron-induced photon emission and local surface structure on atomic and mesoscopic scales. Gimzewski and co-workers reported the first STM-induced photon emission results from rough metal films[8] and more recently with atomic resolution.[9] During this time the issue of photon emission resulting from STM-surface interaction has attracted considerable experimental[8–18] and theoretical interest.[19–22] Despite the extensive effort controversies still exist in regard to the excitation mechanism of photon emission from rough metal surfaces due to the lack of a direct correlation of emission yield with mesoscopic (10–100 nm) surface morphology.

Persson and Baratoff proposed a theory for the photon emission yields from electron tunneling to nanometer size metallic particles.[22] The metallic particle excitation that emits radiation is modeled as a radiative (dipolar) surface plasmon mode. Based on their estimates the two surface plasmon excitation mechanisms, inelastic electron tunneling or hot electron excitation, can be differentiated by their emission probabilities (i.e., $\sim 10^{-3}$ and $\sim 10^{-6}$, respectively) and also particle size dependent emission yield for particles with radii up to a few hundred angstroms. Their paper provides analytical expressions of photon yields associated with the mechanisms for STM-induced emission. Therefore, the size-dependent photon emission yield of metallic particles can be evaluated using appropriate experimental parameters thus facilitating comparison with experiment.

This letter reports the results of STM-induced emission measurements of rough Au films that definitively establish the mechanism of electron-induced photon emission. The experimental findings and theoretical analysis show that: (1) STM topographic images and photon maps possess spatial correlation on nanometer length scales, (2) the absolute emission probability of rough Au films is consistent with the theoretical estimate based on the inelastic tunneling electron-excited surface plasmon model and, most importantly, (3) the experimental results for particle size-dependent emission can be well reproduced by the same model.

The experimental setup is shown in Fig. 1. The STM scanner (Digital Instruments, Bioscope) was mounted on the stage of a modified inverted microscope. Photons emitted from the tunneling gap defined by the STM tip and the sample were collected by a microscope objective (N.A. $=0.75$) beneath the sample, and then detected by a photon-counting system.

The polycrystalline Au films were prepared in high vacuum ($<10^{-6}$ Torr) by thermal evaporation of metal onto microscope cover slips held at room temperature. The thick-

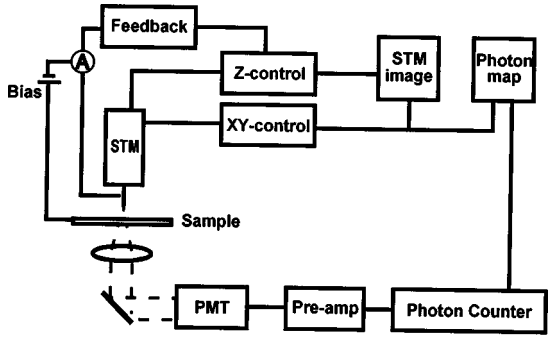

FIG. 1. Experimental schematic. The STM scanner is mounted on the stage of an inverted microscope such that the sample under study is simultaneously accessible by the STM tip and emission collection/detection system (Hamamatsu R2949 PMT, SRS SR400 photon counter). The apparatus is in an electromagnetic and acoustic isolation enclosure and on a rubber mat supported by a vibration isolation table (Newport). The symbol ''A'' represents the pre-amplifier. The measurements are made with a Pt/Ir tip.

a)Author to whom correspondence should be addressed; electronic mail: nscherer@rainbow.uchicago.edu

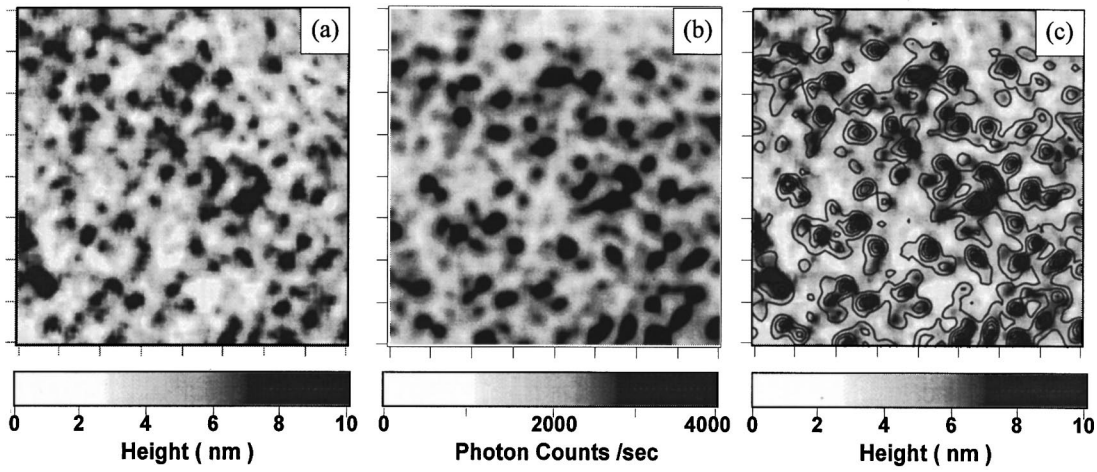

FIG. 2. (a) STM constant current mode image of a 25-nm-thick Au film. The 400×400 nm square image consists of 40 000 pixels and was obtained in ambient conditions with setpoint current=200 pA and bias=2.0 V. (b) Simultaneously measured photon emission map. The photon counting integrating time is 0.1 s per pixel. (c) Overlay of topography [Fig. 2(a)] and contour of photon emission map.

ness of the final Au films is about 25 nm.[23] The STM was operated in constant current mode and the bias was applied to the sample. The *Z* piezo feedback voltages and the photon counts were then recorded simultaneously in a point-by-point fashion and were used to generate topography and photon maps, respectively.

Figure 2(a) shows a representative topographic image of Au films. Interpretating constant-current STM images as surface topography is possible for metallic systems since the local density of electronic states on nanometer to micrometer scales is quite homogeneous.[12,15,16] This was confirmed here by the comparable roughness of the film obtained with atomic force microscopy (AFM; $\text{Roughness}_{\text{RMS}}=2.17$ nm) and STM ($\text{Roughness}_{\text{RMS}}=1.95$ nm). As many as one hundred features, termed particles, can be identified on the image projecting above the otherwise flat background of the surface.[24]

The spatially resolved photon emission intensity of the same area, recorded simultaneously with the STM image of Fig. 2(a), is shown in Fig. 2(b). The maximal emission intensity is about 4000 counts/s for a typical measurement. The Au surface does not emit uniformly and that the important length scale of the luminescent regions is on the order of tens of nanometers which is comparable to the length scale of features observed in the STM topographic image. The correlation of the two data sets is shown in Fig. 2(c) where the photon emission data of Fig. 2(b) is represented as a contour plot overlaid on the STM image of Fig. 2(a). The photon map is well correlated with the film structure seen in the corresponding STM topographic image. The close similarity between the STM images and photon maps in terms of domain (i.e., particle) sizes and shapes is significant for the analysis performed below because it facilitates the unambiguous identification of the ''particles'' in the STM images with the corresponding emitting domains in the photon maps.

The emission probability of rough Au films can be estimated by taking into account the tunneling current, the optical transmittance of the sample/substrate, the light collection efficiency of the microscope objective, and the quantum efficiency of the photomultiplier tube, which are 200 pA, ~20%, 17%, and ~15% (at 600 nm), respectively. The resultant photon creation probability of Au films is determined to be $\sim7\times10^{-4}$ photons per tunneling electron.[25] The theoretically predicted values are $\sim10^{-3}$ for the inelastic tunneling mechanism and of order 10^{-6} for the hot-electron mechanism[22] suggesting that inelastic tunneling is the surface plasmon excitation process.

The data of Fig. 2 and several similar images were analyzed by plotting the emission intensity of each particle against the radius. A flat background reference surface is first established and the protruding area above the reference surface is identified as one particle. The radii of the particles are evaluated by approximating the particles as hemispheres of the same area. The particle sizes range from about 4 to over 60 nm in diameter. The emission intensity of each particle is then obtained by adding the counts from four pixels with the largest values (almost always four contiguous pixels in the center of a particle) within the corresponding domain of the photon map. The results, emission yield versus particle size for three independent measurements, are plotted in Fig. 3. The emission yield shows dramatic particle-size dependence, increasing (nonlinearly) with particle size to a maximum value and turning over.

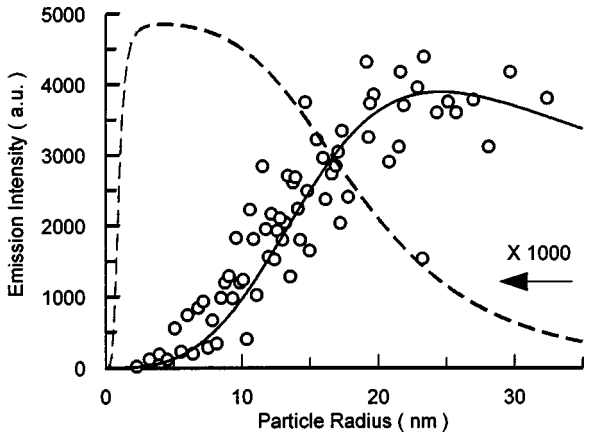

FIG. 3. Particle size-dependence of STM-induced photon emission. The solid and dashed lines are the emission intensity corresponding to inelastic tunneling and hot electron processes calculated from Eqs. (1) and (2), respectively. Note that the dashed line has been multiplied by 1000.

For comparison, the theory of Ref. 22 is used to calculate the size-dependent emission probability of metallic particles**.** The photon yield induced by inelastic tunneling from a metallic particle of radius R is[22]

$$P_{\text{inelastic}}(R)=\left[\frac{\alpha}{8}\right]\left[\frac{\hbar\Omega}{W}\right]\left[\frac{\hbar c/R}{\hbar^2 s^{-2}/2m}\right]\left[1-\frac{\hbar\Omega}{eV}\right]\times\left[1+\frac{3C}{2}\frac{v_F}{c}\left(\frac{\Omega R}{c}\right)^{-4}\right]^{-1}, \quad (1)$$

which includes the probability for an electron to tunnel inelastically by exciting a surface plasmon and the radiative decay rate of a surface plasmon.[26] The solid line in Fig. 3 shows the variation of the emission wavelength-integrated photon yield with the particle radius R, using $s=6$ Å, $W=4$ eV, and eV$=2.5$ eV. The excellent agreement between the model calculation, which has only one fitting parameter C, and the experimental data is persuasive evidence that inelastic tunneling is the principle mechanism responsible for excitation of radiative surface plasmon modes.

The other possible mechanism, hot-electron excitation, can also be evaluated by considering the two competing decay channels of hot electrons, radiative plasmon decay, and nonradiative electron-hole quenching.[22] The associated photon emission yield is given by

$$P_{\text{hot}}(R)=\left[\frac{w}{w'+w}\right]\left[1+\frac{3C}{2}\frac{v_F}{c}\left(\frac{\Omega R}{c}\right)^{-4}\right]^{-1}, \quad (2)$$

where w is the rate for a hot electron in the particle to decay to a lower energy level while exciting a surface plasmon and w' is the quenching rate of a hot electron due to the excitation of an electron-hole pair. They are

$$w=2\sqrt{2}\left[\frac{\varepsilon}{\hbar}\right]\left[\frac{\varepsilon-\hbar\Omega}{\hbar\Omega}\right]^{1/2}\left[\frac{e^2/a_0}{\hbar\Omega}\right]^{5/2}\left[\frac{a_0}{R}\right]^4\times\left[1-\frac{3(\hbar\Omega)^2}{2U[(U-\varepsilon)^{1/2}+(U+\hbar\Omega-\varepsilon)^{1/2}]^2}\right]^2 \quad (3)$$

and

$$w'\approx 0.018\left[\frac{e^2}{a_0\hbar}\right]\left[\frac{\varepsilon}{\varepsilon_F}-1\right]^2, \quad (4)$$

where ε is the energy of the hot electron, ε_F is the Fermi energy, and $U=\varepsilon_F+W$. The result, represented by the dashed line in Fig. 3, is obtained for $\varepsilon=8.0$ eV, $\varepsilon_F=5.5$ eV, and $W=4$ eV. Note that for $R\sim 10-30$ nm the absolute photon yield is ~ 3 orders of magnitude smaller than the emission yield associated with inelastic tunneling[22] and thus its contribution is negligible in the particle size range considered here. Furthermore, the disagreement between the experimental result and the dashed line is obvious. As a result, the possibility of photon emission induced by hot electron injection can be ruled out for several nanometer diameter and larger size particles.

In conclusion, the results of STM-induced photon emission experiments of hemispheroid structured Au films and comparison with model calculations definitively demonstrate that inelastic electron tunneling is the mechanism responsible for photon emission observed in scanning tunneling microscopy. Further studies of metallic particles on nonmetallic dielectric substrates to examine particle–particle plasmon interaction and characterize the photonic properties of mesoscopically structured metal films are underway.

This research was supported by the University of Chicago MRSEC (DMR-9400379), the David and Lucille Packard Foundation, a Camile Dreyfus Teacher-Scholar award, and a Sloan Foundation Fellowship.

[1] H. Raether, *Springer Tracts in Modern Physics*, Vol. 111 (Springer, Heidelberg, 1988).
[2] W. Wang, M. J. Feldstein, and N. F. Scherer, Chem. Phys. Lett. **262**, 573 (1996).
[3] C. K. Chen, A. R. B. de Castro, and Y. R. Shen, Phys. Rev. Lett. **68**, 476 (1981).
[4] M. J. Feldstein, P. Vohringer, W. Wang, and N. F. Scherer, J. Phys. Chem. **100**, 4739 (1996).
[5] C. Douketis, V. M. Shlaev, T. L. Haslett, Z. Wang, and M. Moskovits, J. Electron Spectrosc. Relat. Phenom. **64/65**, 167 (1993).
[6] J. Lambe and S. L. McCarthy, Phys. Rev. Lett. **37**, 923 (1976).
[7] G. Binning, H. Rohrer, C. Gerber, and E. Weibel, Phys. Rev. Lett. **49**, 57 (1982).
[8] J. K. Gimzewski, B. Reihl, J. H. Coombs, and R. R. Schlitter, Z. Phys. B **72**, 497 (1988).
[9] R. Berndt, R. Gaisch, W. D. Schneider, J. K. Gimzewski, B. Reihl, R. R. Schlitter, and M. Tschudy, Phys. Rev. Lett. **74**, 102 (1995).
[10] R. Berndt, J. K. Gimzewski, and P. Johansson, Phys. Rev. Lett. **67**, 3796 (1991).
[11] I. I. Smolyaninov, V. S. Edelman, and V. V. Zavyalov, Phys. Lett. A **158**, 337 (1991).
[12] V. Sivel, R. Coratger, F. Ajustron, and J. Beauvillain, Phys. Rev. B **45**, 8634 (1992).
[13] A. W. McKinnon, M. E. Welland, T. M. H. Wong, and J. K. Gimzewski, Phys. Rev. B **48**, 15250 (1993).
[14] R. Berndt, J. K. Gimzewski, and P. Johansson, Phys. Rev. Lett. **71**, 3493 (1993).
[15] V. Sivel, R. Coratger, F. Ajustron, and J. Beauvillain, Phys. Rev. B **51**, 14598 (1995).
[16] T. Umeno, R. Nishitani, A. Kasuya, and Y. Nishina, Phys. Rev. B **54**, 13499 (1996).
[17] M. J. Feldstein and N. F. Scherer, Proc. SPIE **3272**, 58 (1998).
[18] Y. H. Liau and N. F. Scherer, Proc. SPIE **3273**, 203 (1998).
[19] P. Johansson, R. Monreal, and P. Apell, Phys. Rev. B **42**, 9210 (1990).
[20] Y. Uehara, Y. Kimura, S. Ushioda, and K. Takeuchi, Jpn. J. Appl. Phys., Part 1 **31**, 2465 (1992).
[21] A. Madrazo, M. Nieto-Vesperinas, and N. Garcia, Phys. Rev. B **53**, 3654 (1996).
[22] B. N. J. Persson and A. Baratoff, Phys. Rev. Lett. **68**, 3224 (1992).
[23] Film thickness was determined by a calibrated quartz microbalance.
[24] The root-mean-square roughness of the substrate is measured to be less than 0.6 nm by AFM, hence a small contribution.
[25] To the best of our knowledge, no experimental value of photon creation efficiency for Au films has been reported before.
[26] $\alpha=e^2/\hbar c\approx 1/137$ is the fine-structure constant, e is the electron charge, m is the electron mass, c is the speed of light, s is the separation between the initial and final hybrid states of tunneling electrons extended over the tip and the particle, v_F is the Fermi velocity, Ω is the resonance frequency of the surface plasmon mode of the metal particle, V is the bias voltage, W is the barrier height, and C is a constant. In Ref. 22, the authors indicated that the constant C is on the order of unity; the best fit to the experimental data is obtained with $C=0.5$.